Extended Abstracts of the 2010 International Conference on Solid State Devices and Materials, Tokyo, 2010, pp1120-1121

First-Principles Calculations of Quantum Transport Properties of $Fe/Fe_2VAl/Fe$ Trilayers

Shin Yabuuchi, Isao Kitagawa, Tomoyuki Hamada

Hitachi, Ltd., Advanced Research Laboratory
Akanuma 2520,Hatoyama-machi, Saitama 350-0395, Japan
Phone: +81-49-296-6111 E-mail: shin.yabuuchi.xj@hitachi.com

1. Introduction

Recently, highly sensitive read heads have been required as areal density of hard disk drives (HDDs) has increased. Low-sensor resistance is one of the key factors to achieve highly sensitive sensors [1,2]. There are two types of magnetoresistance (MR) sensors: tunnel magnetoresistive (TMR) sensors, and current-perpendicular-to-plane giant magnetoresistive (CPP-GMR) sensors. To achieve low sensor resistance using a MgO based TMR sensor, a MgO barrier with a thickness of less than four mono-layers (MLs) is strongly needed [3]. However, it has so far been difficult to fabricate a low resistance area (RA) product while maintaining a high TMR ratio. Therefore, the CPP-GMR sensor is expected to perform better than the TMR sensor, since it has lower resistance than that of the TMR sensor. However, the MR ratio of a conventional CPP-GMR sensor is not always high enough. It has been reported that a current-confined-path (CCP) structure is useful for improving the CPP-GMR [4]. The structure is made of a thin insulator with metallic nano-holes that confine the current paths in real space. Thus, it could also be an effective way to confine the conducting channel in the wave vector space using semimetals since the Fermi surface of semimetals quite small.

In this work, we focus on semimetallic Fe_2VAl, which is known as a full-Heusler alloy [5]. We investigated the quantum transport properties of $Fe/Fe_2VAl/Fe$ trilayers using first-principles calculations.

2. Methodology

To obtain the electronic structure and transport properties of the $Fe/Fe_2VAl/Fe$ trilayers, we performed first-principles calculations using the density-functional theory within the generalized gradient approximation (GGA) and the local spin density approximation (LSDA). We used norm-conserving pseudopotentials and a linear combination of pseudo-atomic orbitals for the basis set [6]. Transport properties were evaluated using Green's function method and the Landauer formula. All the calculations were carried out using the OpenMX code [6,7]. We considered Fe_2VAl (100) layers sandwiched by Fe with a (001) surface. Figure 1 is a schematic of the $Fe(001)/Fe_2VAl(001)/Fe(001)$ trilayer structure. The lattice constant of bulk Fe_2VAl and body-centered-cubic (BCC)-Fe are 5.761 Å and 2.866 Å, respectively [5]. To calculate the $Fe/Fe_2VAl/Fe$ trilayer, the lattice constant was fixed at 5.732 Å. We evaluated the RA of trilayer devices using the relationship between the Landauer formula and the transmission at Fermi energy (E_F). To evaluate the MR ratio, we calculated the electronic structure and transmission of the trilayer in the parallel magnetization configuration (PC) and the antiparallel magnetization configuration (APC) of the two Fe leads.

3. Results and Discussion

Figure 2 (a) shows the majority- and minority-spin local density of states (LDOS) of Fe atoms at the boundary of the scattering region. Figure 2 (b) shows the majority- and minority-spin LDOSs of Fe atoms in the center of scattering region. The LDOSs of Fe atoms in the boundary of the scattering region are similar to that of bulk BCC-Fe and show ferromagnetic metallic properties. In Fig. 2 (b), on the other hand, the LDOSs clearly show non-magnetic properties and a low density of states at E_F, indicating semimetallic properties, which suggests that the center of the scattering region maintains the semimetallic properties of bulk Fe_2VAl.

Figure 3 (a) and (b) show the dependence of transmissions at E_F on the in-plane wave vector $k_{||}=(k_x,k_y)$ for the majority- and minority-spin states in the PC, respectively. Peaked structures can be seen around $k_{||}=(0,0)$ and at the edge of the Brillouin zone. These results suggest that the high transmission region in the in-plane wave vector space is confined by the semimetallic Fe_2VAl layer. The $k_{||}$-dependent transmissions originate from a small Fermi surface of the semimetallic Fe_2VAl. Figure 3 (c) shows the $k_{||}$-dependence of transmissions at E_F in the APC. From the averages of the $k_{||}$-dependent transmissions in the PC and the APC, we found that the MR ratio was about 160% at zero bias.

Figure 4 (a) shows the band structure of bulk Fe_2VAl along the [001] direction. Figure 4 (b) and (c) show the transmissions as a function of energy at $k_{||}=(0,0)$ for majority- and minority-spin, respectively. The transmission of majority-spin above E_F is quite low due to the band asymmetry between the Fe leads and Fe_2VAl layers. The transmission of majority-spin around E_F is high because of the phase-matching of the wave function between the localized 3*d* states of Fe_2VAl and the 3*d* states of the Fe leads.

Figure 5 plots the dependence of RA on Fe_2VAl layer thickness in the PC. Figure 5 also shows the dependences of RA on BCC-Cu and MgO layer thickness for reference. We found that the semimetallic Fe_2VAl layers achieved a low RA. Such low a RA is difficult to achieve using ultrathin (~4 ML) MgO insulators. For theFe_2VAl thickness of ~2.5 nm, the RA of the Fe_2VAl layer was ten times higher than that calculated for all-metal (BCC-Cu) CPP-GMR. These results suggest that semimetallic Fe_2VAl layer should be a promising spacer between two ferromagnetic leads for MR sensors with low RAs.

4. Conclusion

We investigated the electronic structure and quantum transport properties of Fe/Fe_2VAl/Fe trilayer structures. We found that the transmission in the in-plane wave vector space was confined by the semimetallic Fe_2VAl layer. The semimetallic Fe_2VAl made it possible to achieve a low RA, which is difficult to achieve using a conventional insulator or metal.

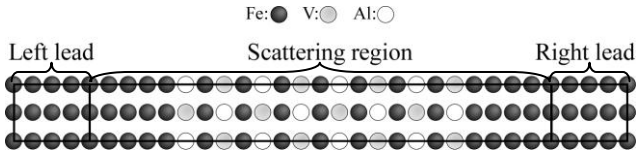

Fig. 1 Schematic illustration of Fe(001)/Fe_2VAl(001)/Fe(001) trilayers

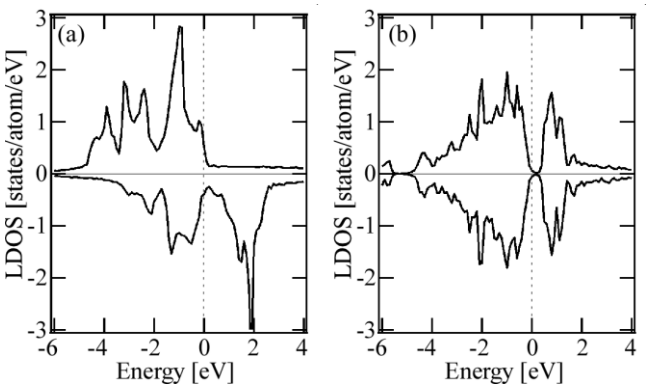

Fig. 2 Local density of states of Fe atoms (a) at the boundary of the scattering region, (b) in the center of the scattering region. The sign of LDOS indicates the majority-spin (positive) and minority-spin (negative) states. E_F is at 0.

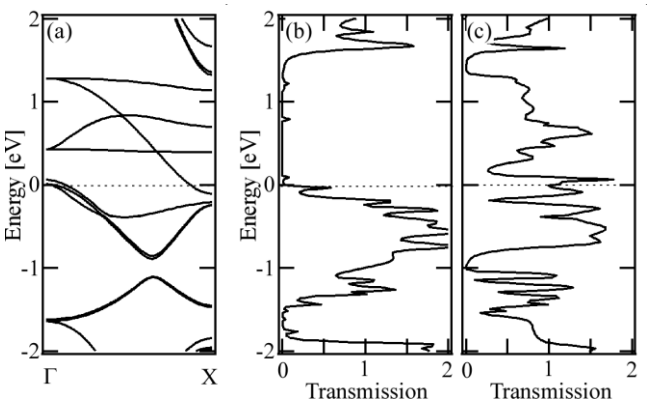

Fig. 4 (a) Band structure of bulk Fe_2VAl along the [001] direction. Transmission as a function of energy at $k_{||}$=(0,0) in the PC for (b) majority-spin and (c) minority-spin. E_F is at 0.

References

[1] M. Takagishi, et al.,IEEE Trans. Mag. **38**, (2002) 2277.
[2] H. Katada, et al., J. Mag. Mag. Mat. **320**, (2008) 2975.
[3] S. Isogami, et al.,Appl. Phys. Lett. **93**, (2008) 192109.
[4] H. Fukuzawa, et al., Appl. Phys. Lett. **87**, (2005) 082507.
[5] R. Weht and W. E. Pickett, Phys. Rev. B **53**, (1998) 6855.
[6] T. Ozaki, et al., Phys. Rev. B **81**, (2010) 035116.
[7] http://www.openmx-square.org/

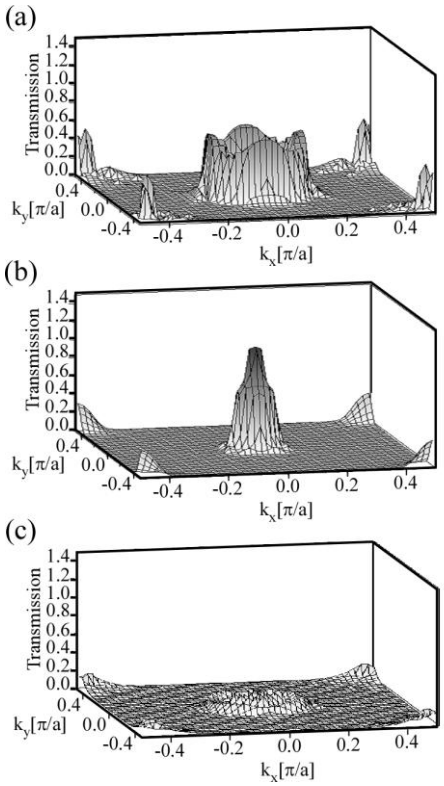

Fig. 3 The dependence on in-plane wave vector $k_{||}$=(k_x,k_y) of transmissions at E_F for (a) the majority-spin states in the PC, (b) minority-spin states in the PC, and (c) the majority- or minority-spin state in APC.

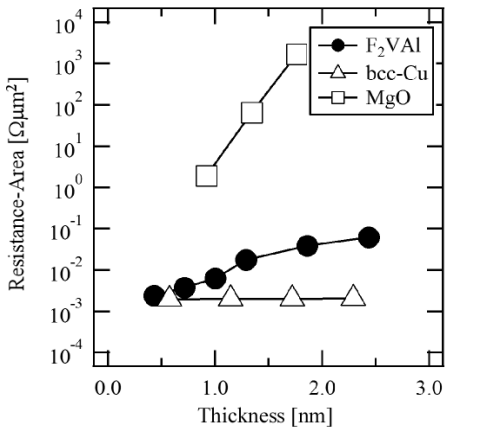

Fig. 5 Dependence of RA on Fe_2VAl layer thickness (circles), BCC-Cu layer thickness (open triangles), and MgO layer thickness (open squares) in the PC.